Journal of Catalysis 277 (2011) 164–172

Contents lists available at ScienceDirect

Journal of Catalysis

journal homepage: www.elsevier.com/locate/jcat

Decamethylosmocene-catalyzed efficient oxidation of saturated and aromatic hydrocarbons and alcohols with hydrogen peroxide in the presence of pyridine ☆

Georgiy B. Shul'pin [a,*], Marina V. Kirillova [b], Yuriy N. Kozlov [a], Lidia S. Shul'pina [c], Alexander R. Kudinov [c], Armando J.L. Pombeiro [b]

[a] *Semenov Institute of Chemical Physics, Russian Academy of Sciences, ulitsa Kosygina, dom 4, Moscow 119991, Russia*
[b] *Centro de Química Estrutural, Complexo I, Instituto Superior Técnico, TU Lisbon, Av. Rovisco Pais, 1049-001 Lisbon, Portugal*
[c] *Nesmeyanov Institute of Organoelement Compounds, Russian Academy of Sciences, ulitsa Vavilova, dom 28, Moscow 119991, Russia*

ARTICLE INFO

Article history:
Received 2 July 2010
Revised 3 November 2010
Accepted 5 November 2010
Available online 9 December 2010

Keywords:
Alcohols
Alkanes
Benzene
C–H functionalization
Homogeneous catalysis
Hydrogen peroxide
Metallocenes
Osmium complexes

ABSTRACT

Decamethylosmocene, $(Me_5C_5)_2Os$ (**1**), is a pre-catalyst in a very efficient oxidation of alkanes with hydrogen peroxide in acetonitrile at 20–60 °C. The reaction proceeds with a substantial lag period that can be reduced by the addition of pyridine in a small concentration. The lag period can be removed if **1** is incubated with pyridine and/or H_2O_2 in MeCN prior to the alkane oxidation. Alkanes, RH, are oxidized primarily to the corresponding alkyl hydroperoxides, ROOH. Turnover numbers attain 51,000 in the case of cyclohexane (maximum turnover frequency was 6000 h^{-1}) and 3600 in the case of ethane. The oxidation of benzene and styrene also occurs with a lag period to afford phenol and benzaldehyde, respectively. A kinetic study of cyclohexane oxidation and selectivity parameters (measured in the oxidation of *n*-heptane, methylcyclohexane, isooctane, *cis*- and *trans*-dimethylcyclohexanes) indicates that the oxidation of saturated, olefinic, and aromatic hydrocarbons proceeds with the participation of hydroxyl radicals. The **1**/H_2O_2/py/MeCN system also oxidizes 1-phenylethanol to acetophenone.

1. Introduction

The development of new catalysts that are capable to transform hydrocarbons and other organic compounds efficiently and selectively under mild conditions (at temperature <100 °C) and under the action of green oxidants (molecular oxygen, hydrogen peroxide) constitutes a challenge to various areas of modern chemistry and, in particular, to catalysis. Complexes of transition metals catalyze oxidations of various organic compounds [1], including alcohols [2–5], aromatic [6,7], olefinic [8–15], and saturated [16–21] hydrocarbons by molecular oxygen, peroxides, and some other oxidizing reagents. Organometallic compounds (like, for example, the quite carefully studied methyltrioxorhenium, MTO) only seldom play the role of pre-catalysts in oxidations of organic compounds [22–27].

Oxo complexes of osmium have been reported to efficiently catalyze dihydroxylation of olefins with peroxides [28,29]. In contrast, relatively small number of publications has been devoted to osmium-catalyzed oxidations of alcohols [30–32] and saturated and aromatic hydrocarbons [32–42]. In the present work, we demonstrate for the first time that decamethylosmocene (**1**) is a very efficient catalyst for the oxidation of hydrocarbons and alcohols by hydrogen peroxide if pyridine in a low concentration is present in the solution.

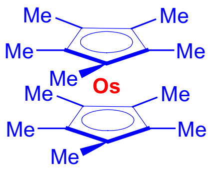

1

2. Results and discussion

We have found that heating a solution of an alkane (typically cyclohexane) in acetonitrile with hydrogen peroxide and decamethylosmocene **1** affords alkyl hydroperoxide as the main primary product with a turnover number (TON, moles of products per one mol of the catalyst) up to 750 after 6 h (Fig. 1, curve 1). Alkyl hydroperoxide decomposes partly in the course of the oxidation

---

☆ Part 3 from the series "Oxidations Catalyzed by Osmium Compounds". For Parts 1 and 2, see Refs. [36] and [32], respectively.

[*] Corresponding author.
E-mail addresses: shulpin@chph.ras.ru, gbsh@mail.ru (G.B. Shul'pin).

0021-9517/$ - see front matter © 2010 Elsevier Inc. All rights reserved.
doi:10.1016/j.jcat.2010.11.002

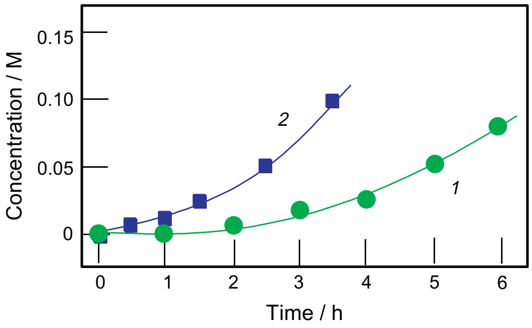

Fig. 1. Accumulation of oxygenates (predominantly cyclohexyl hydroperoxide) with time in cyclohexane oxidation with H_2O_2 catalyzed by complex **1** in the absence of pyridine in acetonitrile. Conditions (curve 1): $[\mathbf{1}]_0 = 1 \times 10^{-4}$ M, [cyclohexane]$_0$ = 0.91 M, $[H_2O_2]_0$ = 2.2 M, $[H_2O]_{total}$ = 4.2 M, 50 °C. Curve 2: a mixture of **1** (5×10^{-5} M), H_2O_2 (2.2 M), and water ($[H_2O]_{total}$ = 4.2 M) and acetonitrile was incubated at 50 °C during 1 h, whereafter cyclohexane (0.91 M) was added at the time = 0 h.

reaction to give the corresponding ketone and alcohol. Concentrations of the three products were measured by GC analysis comparing concentrations of cyclohexanone and cyclohexanol before and after reduction of the reaction mixture with an excess of PPh_3. For this method, developed previously by some of us, see Refs. [18,32,41,43,44]. The product accumulation proceeds with autoacceleration, and this testifies that compound **1** is only a catalyst precursor, which is transformed in the course of the process into a catalytically active species. The formation of this species occurs under the action of hydrogen peroxide and apparently acetonitrile. Indeed, if a solution of **1** and H_2O_2 is incubated during 1 h and cyclohexane is added only after this incubation the oxidation proceeds (Fig. 1, curve 2) noticeably faster (TON = 1000 after 3.5 h).

If pyridine in a low concentration is added, the lag period of the oxygenation becomes much shorter (Fig. 2, curve 1) and TON attains 3600. In the presence of Cl_3CBr, the reaction affords a considerable amount of cyclohexyl bromide (Fig. 2, curve 2), which indicates the generation of alkyl radicals as transient species. Preliminary incubation of the solution of **1**, H_2O_2, H_2O, and pyridine with subsequent addition of cyclohexane (Fig. 2, curve 3) or of the solution of **1**, cyclohexane, and pyridine with subsequent addition of H_2O_2 (Fig. 2, curve 4) almost removes the lag period. This period is not noticed also when a solution containing **1**, H_2O_2, water, and acetonitrile was incubated during 1 h prior to the addition of cyclohexane and pyridine (Fig. 3). In this experiment, a TON of 3800 was attained after 4 h. It can be concluded that a catalytically active species is formed relatively quickly under the action of H_2O_2 and/or pyridine on the pre-catalyst **1**. It is reasonable to assume that this species is generated after removing one or two pentamethylcyclopentadienyl ligands from complex **1**. These ligands are apparently replaced by pyridine, water, and acetonitrile.

Kinetic curves of the oxygenate accumulation at three different initial concentrations of the pre-catalyst **1** are shown in Fig. 4. It is clear that for the three concentrations of **1,** the maximum attained oxidation rates W_{max} at $[\mathbf{1}]_0 \geqslant 1 \times 10^{-4}$ M (calculated from the slope of the corresponding dotted lines in Fig. 4) are practically equal. The lag period is shorter at $[\mathbf{1}]_0 = 2 \times 10^{-4}$ and 3×10^{-4} than at 1×10^{-4} M.

We were able to attain extremely high TON values when very low concentrations of the pre-catalyst **1** were used (Fig. 5). Thus, in the cyclooctane oxidation, TON = 20,000 after 12 h (Fig. 5, curve 3*b*), and in the cyclohexane oxygenation, TON = 50,000 after 15 h (Fig. 5, curve 4*a*). The oxidation efficiently occurs at 20 and 70 °C (Fig. 6). The catalase activity (the non-productive decomposition of H_2O_2 to O_2 and H_2O) of the system, which accompanies the alkane oxygenation is noticeably lower at room temperature. In this case, the yield of oxygenates was 44% after 16 days based on the starting cyclohexane

It is interesting that the maximum reaction rate W_{max} increases when the total concentration of water in the reaction solution grows from 2.1 to 5.9 M. The dependence of W_{max} on water concentration has a maximum (Fig. 7). As it was mentioned above (see Fig. 4), there is a plateau in the curve, which describes the dependence of W_{max} on the initial concentration of the pre-catalyst **1** at its concentration $\geqslant 1 \times 10^{-4}$ M (Fig. 8). The dependence of W_{max} on the initial concentration of hydrogen peroxide at constant

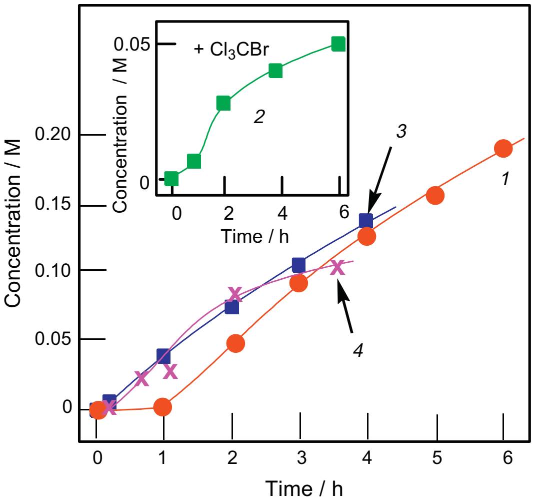

Fig. 2. Accumulation of oxygenates (predominantly cyclohexyl hydroperoxide) with time in cyclohexane oxidation with H_2O_2 catalyzed by complex **1** in the presence of pyridine in acetonitrile. Curve 1: conditions: $[\mathbf{1}]_0 = 5 \times 10^{-5}$ M, [cyclohexane]$_0$ = 0.91 M, $[H_2O_2]_0$ = 2.2 M, $[H_2O]_{total}$ = 4.2 M, [py] = 0.1 M, 50 °C. Curve 2: formation of cyclohexyl bromide in the reaction under conditions of the experiment shown by curve 1, but in the presence of Cl_3CBr (0.5 mL). Curve 3: the solution containing **1** (5×10^{-5} M), H_2O_2 (2.2 M), H_2O (4.2 M), and pyridine (0.1 M) was incubated in acetonitrile at 50 °C during 1 h, whereafter cyclohexane was added at the time = 0 h. Curve 4: the solution containing **1** (5×10^{-5} M), cyclohexane (0.91 M), pyridine (0.1 M), and acetonitrile was incubated at 50 °C during 160 min, whereafter H_2O_2 (2.2 M) containing water ($[H_2O]_{total}$ = 4.2 M) was added at the time = 0 h.

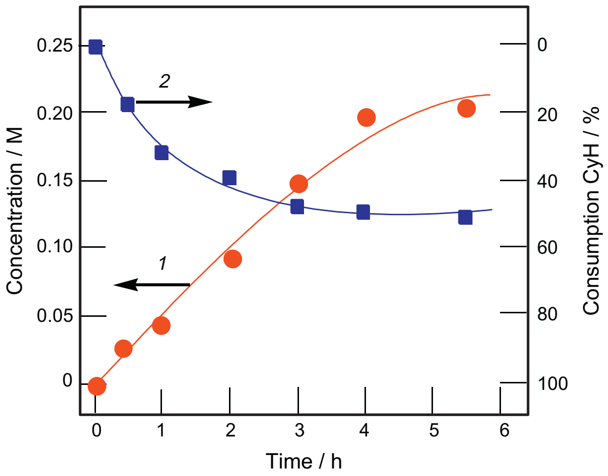

Fig. 3. Accumulation of oxygenates (curve 1; predominantly cyclohexyl hydroperoxide) and consumption of cyclohexane (curve 2) with time in the cyclohexane oxidation with H_2O_2 catalyzed by complex **1** in the presence of pyridine in acetonitrile. The solution containing **1** (5×10^{-5} M), H_2O_2 (2.2 M) with water ($[H_2O]_{total}$ = 4.2 M) and acetonitrile was incubated at 50 °C during 1 h. After that cyclohexane (0.91 M) and pyridine (0.1 M) were added at the time = 0 h.

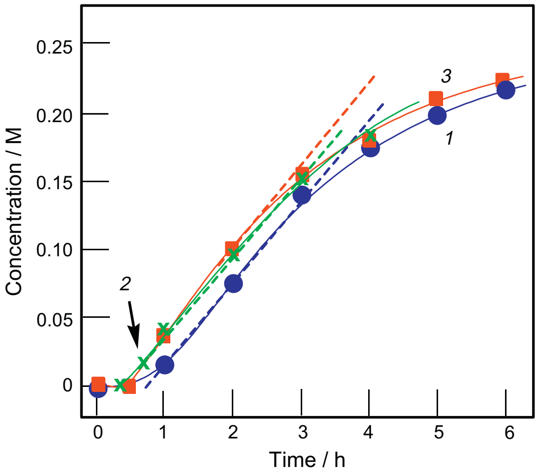

Fig. 4. Accumulation of oxygenates (predominantly cyclohexyl hydroperoxide) with time in cyclohexane oxidation with H_2O_2 catalyzed by complex **1** in the presence of pyridine in acetonitrile. Conditions: $[\mathbf{1}]_0 = 1 \times 10^{-4}$ (curve 1), 2×10^{-4} (curve 2), and 3×10^{-4} M (curve 3), $[\text{cyclohexane}]_0 = 0.91$ M, $[H_2O_2]_0 = 2.2$ M, $[H_2O]_{total} = 4.2$ M, [py] = 0.1 M, 50 °C, total volume of the reaction solution was 5 mL.

concentration of water is reflected with a S-shaped curve (Fig. 9B). The dependence of the initial hydrocarbon oxidation rate on the initial cyclohexane concentration (Fig. 10B) exhibits a plateau when $[\text{cyclohexane}]_0 > ca.$ 0.4 M. Kinetic curves of oxygenate accumulation at different concentrations of added pyridine are shown in Fig. 11. It can be seen that the time period after which the maximum oxidation rate is achieved decreases with increasing pyridine concentration.

The results of Table 1 demonstrate that when the pre-catalyst **1** is used in a very low concentration (1×10^{-6} M), the TONs for alkane oxidation attain extremely high values (up to 51,000, entries 2 and 10). It can also be seen that in the absence of **1** only negligible amounts of the oxygenates are formed (entries 4–7, 11). When the reaction was carried out in an oxygen atmosphere, instead of air, the yield of oxygenates was noticeably higher (compare entries 1 and 8). On the contrary, the oxidation in a CO_2 atmosphere gave three times less amount of product (compare entries 8 and 12). It should be noted that when the reaction was carried out in a CO_2 atmosphere, some amount of molecular oxygen was present in the autoclave and O_2 was also derived from the aqueous hydrogen peroxide solution and *via* the catalase decomposition of H_2O_2. Thus, we can conclude that the formation of oxygenates proceeds with the participation of molecular oxygen present in the reaction vessel.

We have also found that light gaseous alkanes can be oxidized by the system under consideration (Table 2). A comparison of the oxygenate concentrations before and after reduction with PPh_3 indicates that after 24 h at 50 °C, some amounts of isomeric alkyl hydroperoxides are present in the reaction mixture because the concentrations of the alcohols determined by GC increase after the reduction. A significant amount of acetic acid is formed from *n*-butane apparently *via* C–C bond splitting. In the cases of propane and methane, acetic acid is present in low concentration and is formed *via* hydrolysis of acetonitrile.

We measured selectivity parameters in the oxidations of *n*-heptane, branched and cyclic alkanes (Table 3). The regioselectivity parameter determined for the oxidation of *n*-heptane is C(1):C(2):C(3):C(4) = 1:7:7:7. This value is close to those determined previously for systems that oxidize alkanes with the participation of hydroxyl radicals (compare with the parameters summarized in entries 2–9 of Table 3). The corresponding selectivity parameters for the systems that do not involve active hydroxyl radicals (entries 10–15) are noticeably higher. The bond-selectivity parameters (1°:2°:3°) in the oxidation of methylcyclohexane and isooctane by the $\mathbf{1}/H_2O_2$/py system are also close to those found for the systems oxidizing alkanes with the participation of hydroxyl radicals (compare with the parameters summarized in entries 2–9 of Table 3). The oxidation of *cis-* and *trans*-1,2-dimethylcyclohexanes proceeds non-stereoselectively as the *trans/cis* ratios of the isomeric alcohols (after reduction with PPh_3) are *ca.* 1 (Table 3).

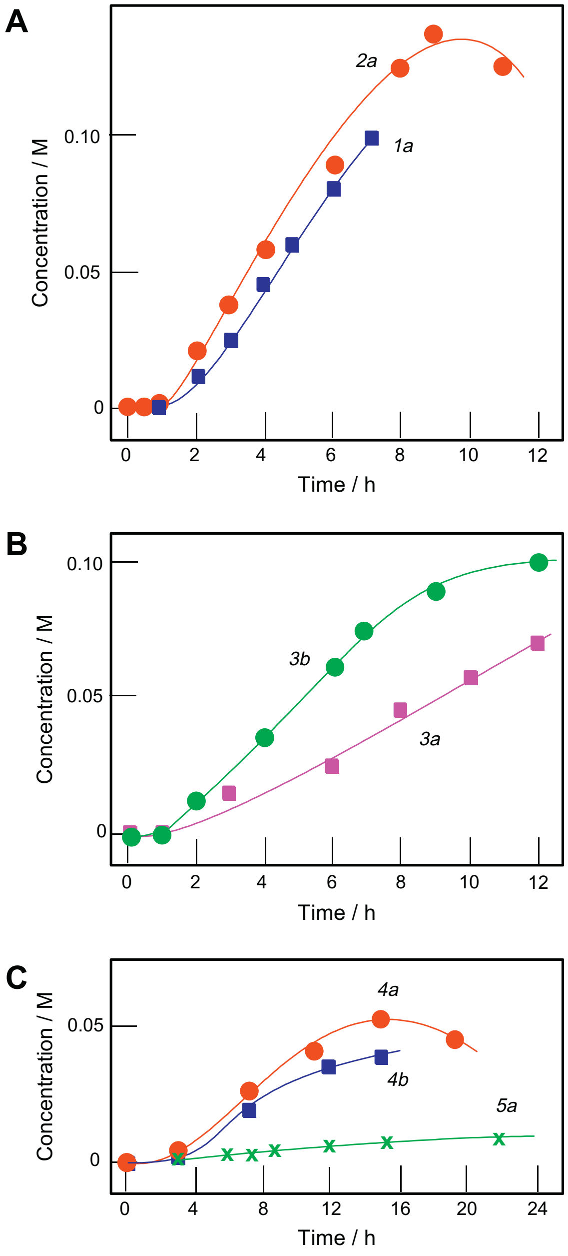

Fig. 5. Accumulation of oxygenates (predominantly alkyl hydroperoxides) with time in oxidation of cycloalkanes (cyclohexane, curve *a*, and cycloctane, curve *b*) with H_2O_2 catalyzed by complex **1** at its different concentrations in the presence of pyridine in acetonitrile. Conditions. Graph A: $[\mathbf{1}]_0 = 1 \times 10^{-5}$ M, $[\text{cyclohexane}]_0 = 0.91$ (curve 1*a*) and 0.46 M (curve 2*a*). Graph B: $[\mathbf{1}]_0 = 5 \times 10^{-6}$ M, $[\text{cycloalkane}]_0 = 0.91$ M. Graph C: $[\mathbf{1}]_0 = 1 \times 10^{-6}$ M for curve 4 and $[\mathbf{1}]_0 = 0$ M for curve 5*a*, $[\text{cycloalkane}]_0 = 0.91$ M. Other conditions for all curves: $[H_2O_2]_0 = 2.2$ M, $[H_2O]_{total} = 4.2$ M, [py] = 0.1 M, 50 °C.

A mechanistic interpretation of the obtained kinetic results on the alkane oxidation is given below. In this context, we stress that the oxygenate accumulation with time occurs with an auto-accel-

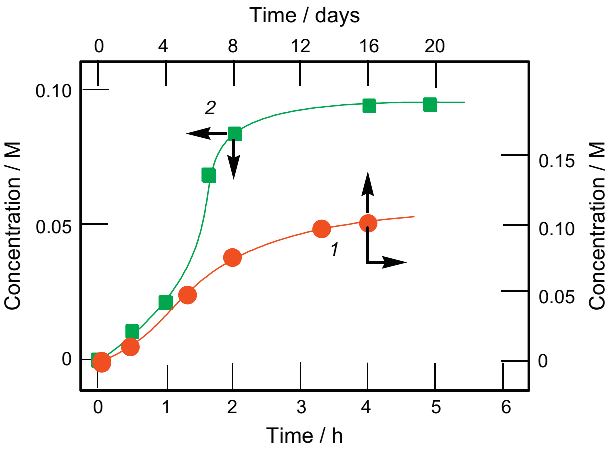

Fig. 6. Accumulation of oxygenates (predominantly cyclohexyl hydroperoxide) with time in cyclohexane oxidation with H_2O_2 catalyzed by complex **1** in the presence of pyridine in acetonitrile at different temperatures: 20 (curve 1; $[cyclohexane]_0 = 0.23$ M, $[H_2O_2]_0 = 1.1$ M, $[H_2O]_{total} = 2.1$ M,) and 70 °C (curve 2; $[cyclohexane]_0 = 0.91$ M, $[H_2O_2]_0 = 2.2$ M, $[H_2O]_{total} = 4.2$ M). Other conditions for both curves: $[\mathbf{1}]_0 = 1 \times 10^{-5}$ M, [py] = 0.1 M.

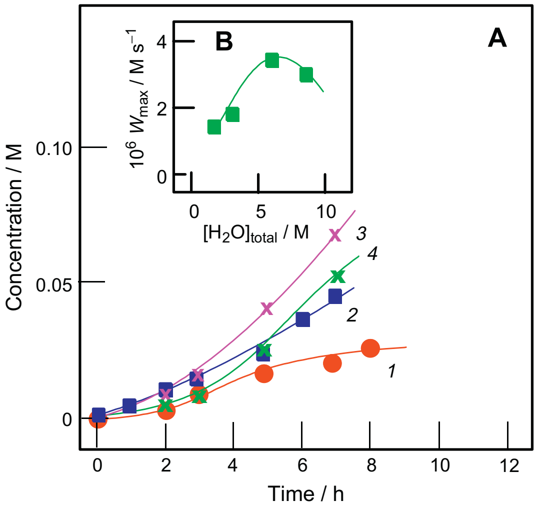

Fig. 7. Graph A: accumulation of oxygenates (predominantly cyclohexyl hydroperoxide) with time in cyclohexane oxidation with H_2O_2 catalyzed by complex **1** in the presence of pyridine in acetonitrile at different concentrations of total water $[H_2O]_{total}$: 2.1 (curve 1), 4.0 (curve 2), 5.9 (curve 3), and 7.7 M (curve 4). Conditions: $[\mathbf{1}]_0 = 1 \times 10^{-5}$ M, $[cyclohexane]_0 = 0.23$ M, $[H_2O_2]_0 = 1.1$ M, [py] = 0.1 M, 50 °C, total volume of the reaction solution was 5 mL. Graph B: dependence of the maximum oxidation rate (calculated from the data shown in graph A) on the total concentration of water.

eration both in the absence and in the presence of pyridine (see curve 1 in Figs. 1 and 2). The lag period (that is the time period before the maximum rate is attained) is shorter if pyridine is added, and it is negligible if the pre-catalyst **1** is incubated in the reaction mixture; whereafter, the oxidation process is initiated by the addition of either H_2O_2 or cyclohexane (see Figs. 1 and 2). These results indicate that in the experiment without preliminary incubation, the formation of an osmium-containing active catalyst form occurs by the reaction between **1** and hydrogen peroxide or pyridine and apparently also acetonitrile. Thus, we can conclude that **1** is only a catalyst precursor that is slowly transformed under the reaction conditions into a catalytically active species. The maximum accumulation rates in the presence and in the absence of pyridine are close (compare curve 2 in Fig. 1 and curve 1 in Fig. 4). Pyridine does not therefore affect the catalytic activity of the oxidizing species generated from **1**. The main effect of pyridine is shortening the lag period and the time for reaching the maximum oxidation rate. This means that the role of pyridine is to accelerate the transformation of **1** into the catalytically active species.

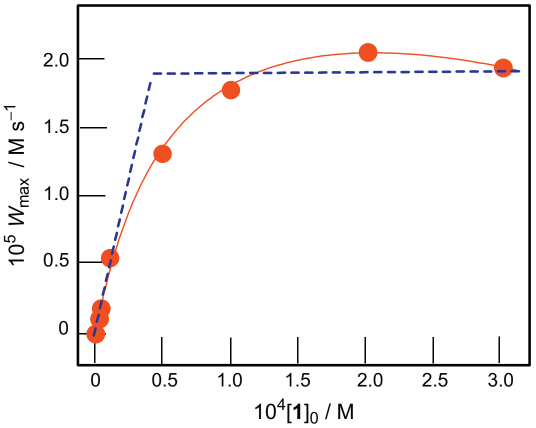

Fig. 8. Dependence of the maximum reaction rate of the cyclohexane oxidation on the initial concentration of pre-catalyst **1**. Conditions: $[cyclohexane]_0 = 0.91$ M, $[H_2O_2]_0 = 2.2$ M, $[H_2O]_{total} = 4.2$ M, [py] = 0.1 M, 50 °C. For the dotted line, see text.

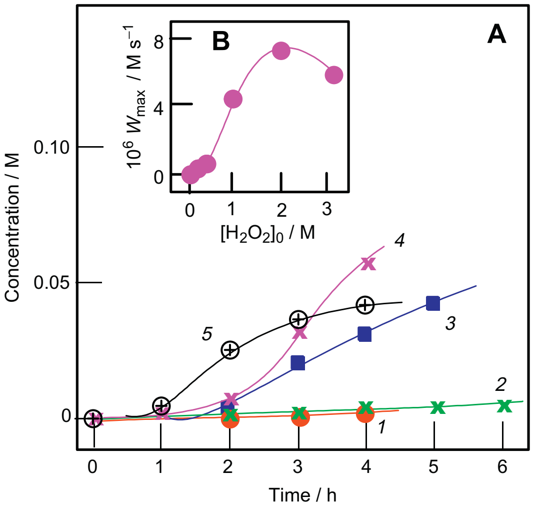

Fig. 9. Graph A: accumulation of oxygenates (predominantly cyclohexyl hydroperoxide) with time in cyclohexane oxidation with H_2O_2 catalyzed by complex **1** in the presence of pyridine in acetonitrile at $[H_2O]_{total}$ = *const* = 5.9 at different concentrations of H_2O_2: 0.25 (curve 1), 0.5 (2), 1.1 (3), 2.0 (4), and 3.1 M (5). Conditions: $[\mathbf{1}]_0 = 5 \times 10^{-5}$ M, $[cyclohexane]_0 = 0.46$ M, [py] = 0.1 M, 50 °C. Graph B: dependence of the maximum reaction rate of the oxidation (calculated from the data shown in graph A) on the initial concentration of H_2O_2.

The selectivity parameters determined for the oxidation of certain alkanes by the $\mathbf{1}/H_2O_2$/py/MeCN system (see Table 3) indicate that this system oxidizes alkanes with the participation of hydroxyl radicals. The kinetic data shown in Fig. 10 are in agreement with this. The dependence of the maximum catalytic reaction rate on the cyclohexane initial concentration (with a plateau, Fig. 10B) testifies that the oxidizing species competitively interacts with the alkane and other components of the reaction solution. Indeed, hydroxyl radicals in the system under consideration can react (in addition to the alkane) with components Y that can be any of the following species: solvent CH_3CN (see Refs. [61,62]), oxidant H_2O_2, pre-catalyst **1**, and catalytically active species *cat*. The kinetic scheme for this case is the following one:

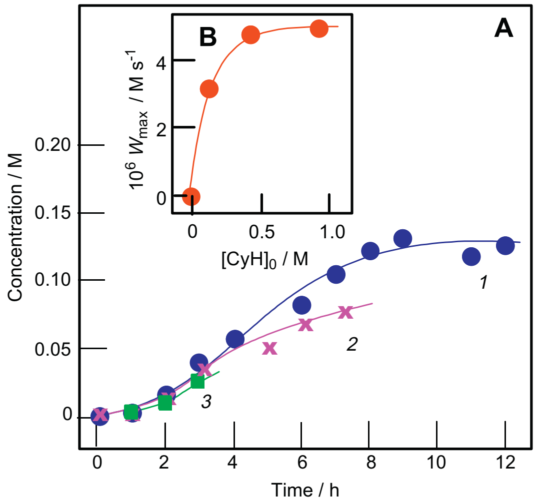

Fig. 10. Graph A: accumulation of oxygenates (predominantly cyclohexyl hydroperoxide) with time in cyclohexane oxidation with H_2O_2 catalyzed by complex **1** in the presence of pyridine in acetonitrile at different concentrations of cyclohexane: 0.92 (curve 1), 0.46 (2), 0.23 (3) M. Conditions: $[\mathbf{1}]_0 = 1 \times 10^{-5}$ M, $[H_2O_2]_0 = 2.2$ M, $[H_2O]_{total} = 4.2$ M, [py] = 0.1 M, 50 °C, total volume of the reaction solution was 5 mL. Graph B: dependence of the maximum reaction rate of the oxidation (calculated from the data shown in graph A) on the initial concentration of cyclohexane.

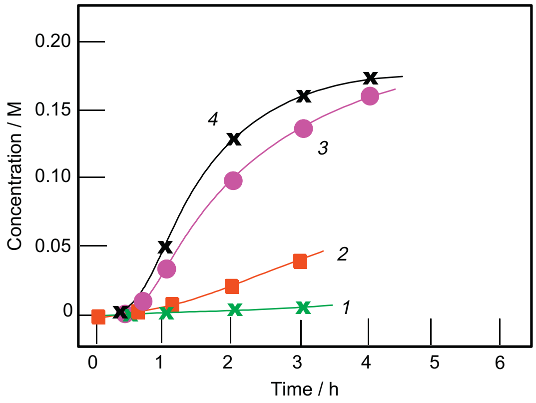

Fig. 11. Accumulation of oxygenates (predominantly cyclohexyl hydroperoxide) with time in the cyclohexane oxidation with H_2O_2 catalyzed by complex **1** in the presence of pyridine in acetonitrile at different concentrations of pyridine: 0.0 (curve 1), 0.01 (2), 0.05 (3), and 0.10 M (4). Conditions: $[\mathbf{1}]_0 = 2 \times 10^{-4}$ M, $[H_2O_2]_0 = 2.2$ M, $[H_2O]_{total} = 4.2$ M, $[\text{cyclohexane}]_0 = 0.91$ M, 50 °C, total volume of the reaction solution was 5 mL.

$$H_2O_2 + cat \rightarrow HO^{\cdot} \quad W_i \tag{i}$$

$$HO^{\cdot} + \text{cyclohexane} \rightarrow \ldots \rightarrow \text{oxygenates} \quad k_1 \tag{1}$$

$$HO^{\cdot} + Y \rightarrow \text{products} \quad k_2 \tag{2}$$

In this scheme, (i) is the effective reaction of hydroxyl radical generation and W_i is the rate of this reaction. Reaction (i) is the rate limiting step in the alkane oxidation. It should be noted that in the sequence of transformations of the alkane into the oxygenates in accordance with Eq. (1), the rate limiting stage is the interaction of hydroxyl radical with the alkane.

Based on the literature data [45,63], the estimate of the rate constants of pseudo-first order for the interaction between HO· and components Y under our conditions led to the following results:

$$k(HO^{\cdot} + CH_3CN)[CH_3CN] \approx (0.6 \div 3.6) \times 10^8 \ s^{-1}$$

$$k(HO^{\cdot} + H_2O_2)[H_2O_2] \leqslant 6 \times 10^7 \ s^{-1},$$

$$k(HO^{\cdot} + cat)[cat] \leqslant 2 \times 10^6 \ s^{-1}.$$

The last value was obtained assuming $k(HO^{\cdot} + cat) \approx 10^{10}$ M^{-1} s^{-1} (which is the characteristic value for a diffusion-controlled reaction) and $[cat] = 2 \times 10^{-4}$ M. It follows from these results that hydroxyl radicals react with acetonitrile in the most efficient way in comparison with the other components Y. Hence, in order to interpret properly the data shown in Fig. 10, we need to take into account only the interactions between hydroxyl radicals and the alkane and acetonitrile. The analysis of the kinetic scheme (i), (1), (2) based on this conclusion led to the following expression for the rate of the oxygenate formation:

$$W_{max} = -\frac{d[\text{cyclohexane}]}{dt} = \frac{W_i}{1 + \frac{k_2[CH_3CN]}{k_1[\text{cyclohexane}]}} \tag{3}$$

It follows from Eq. (3) that the maximum rate of the oxygenate formation corresponds to W_i and is attained at $k_2[CH_3CN] \ll k_1[\text{cyclohexane}]$. At the same time, the oxygenate formation rate that is equal to half of the maximum rate ($W_i/2$) can be reached at $k_2[CH_3CN]/k_1[\text{cyclohexane}] = 1$. The results shown in Fig. 10B demonstrate that half of the maximum oxygenate formation rate is attained at $[\text{cyclohexane}]_0 = 0.1 \div 0.2$ M and $[CH_3CN] \approx 18$ M. As a result, in the frames of our model, we obtain the ratio $k_2/k_1 = (0.55 \div 1.1) \times 10^{-2}$, which is in agreement with the parameters measured for the cyclohexane oxygenation in acetonitrile induced by hydroxyl radicals generated in the H_2O_2 photolysis (0.8×10^{-2}) [45]. The parameter is also in agreement with the results of calculations based on the absolute rate constants for the reactions of hydroxyl radicals with acetonitrile and cyclohexane: $(0.35 \div 2) \times 10^7$ M^{-1} s^{-1} and $(0.9 \div 1.5) \times 10^9$ M^{-1} s^{-1}, respectively [63]. Thus, the kinetic data from Fig. 10B support our assumption that the alkane oxygenation in our system is induced by hydroxyl radicals.

Fig. 8 demonstrates an unusual mode of dependence of the homogeneous catalytic oxidation rate on the initial concentration of the pre-catalyst **1**: the reaction rate W_{max} is proportional to $[\mathbf{1}]_0$ at low concentration of the pre-catalyst, but does not depend on $[\mathbf{1}]_0$ at its relatively high concentration. Proportional dependence of W_{max} on $[\mathbf{1}]_0$ means that a catalytically active species is a monomeric complex of osmium, which is formed from the precursor **1** during the lag period. Independence of W_{max} on $[\mathbf{1}]_0$ at concentration $[\mathbf{1}]_0 > 1 \times 10^{-4}$ M (see Fig. 8) indicates that the rate of the catalytically active species formation is constant under our conditions. The simplest explanation of that unusual behavior is the following one. Under the conditions of our experiments, a sparingly soluble (in aqueous acetonitrile) osmium derivative would be formed. The amount of this osmium compound $>1 \times 10^{-4}$ M leaves this homogeneous solution into another phase that is inactive in the alkane oxidation. As a result, the concentration of the osmium compounds present in the homogeneous solution would be constant and close to 1×10^{-4} M. Let us assume additionally that only a soluble osmium derivative is the catalytically active species and the oxidation rate is proportional to its concentration, what is indicated by the linear segment of the dependence of W_{max} on $[\mathbf{1}]_0$ at $[\mathbf{1}]_0 < 1 \times 10^{-4}$ M (see Fig. 8). In this case, we should find linear growth of W_{max} in the interval $0 < [\mathbf{1}]_0 < 1 \times 10^{-4}$ and independence of W_{max} on $[\mathbf{1}]_0$ at $[\mathbf{1}]_0 \geqslant 1 \times 10^{-4}$ M. This assumption is in agreement with the data shown in Fig. 8 where the expected dependence of W_{max} on $[\mathbf{1}]_0$ is presented by the dotted line.

The observed dependence of W_{max} on $[H_2O_2]_0$ (see Fig. 9B) does not apparently reflect the competitive reaction of the hydroxyl radicals with cyclohexane and hydrogen peroxide. Indeed, as it follows

Table 1
Cyclohexane oxidation.[a]

Entry	Atmosphere	**1** (M)	Time (h)	-one	-ol	Sum	TON
1	Air[b]	5×10^{-5}	4			0.125	2500
2	Air[c]	1×10^{-6}	15			0.051	47,000[e]
3			19			0.045	
4	Air[d]	0	7	0.0006	0.0013	0.0019	–
5			15	0.0015	0.0024	0.0039	–
6			22	0.0010	0.0039	0.0049	–
7			28	0.0013	0.0041	0.054	–
8	O_2	5×10^{-5}	4	0.024	0.150	0.174	3480
9	O_2	5×10^{-6}	24	0.020	0.178	0.198	39,600
10	O_2	1×10^{-6}	24	0.006	0.049	0.055	51,000[e]
11	O_2	0	20	0.0009	0.003	0.004	–
12	CO_2	5×10^{-5}	4	0.020	0.039	0.059	1180

[a] Concentrations (M) of cyclohexanone (-one) and cyclohexanol (-ol) were determined after reduction of the reaction samples with PPh_3. Conditions: $[\text{cyclohexane}]_0 = 0.91$ M, $[H_2O_2]_0 = 2.2$ M, $[H_2O]_{total} = 4.2$ M, [py] = 0.1 M, 4 h at 50 °C. Pressure O_2 1.5 atm, CO_2 3 atm, entries 2–6 were carried out in Teflon-lined autoclaves (total volume 39 mL, volume of the reaction solution was 5 mL). Experiments in air were carried out in an open vessel (1 atm of air), and the volume of the reaction solution was 5 mL.

[b] For this experiment, see Fig. 2, curve 1.

[c] For this experiment, see Fig. 5, curve 4*a*.

[d] For this experiment, see Fig. 5, curve 5*a*.

[e] TON was calculated after subtracting the amount of oxygenates formed in the reaction in the absence of **1**.

Table 2
Oxidation of gaseous alkanes.[a]

Entry	Alkane	Pressure (atm)	Amount (mmol)	Products[b] (M)	TON	Yield[c] (%)
1	*n*-Butane	1	1.4	MeCOEt (0.0147; 0.011), MeCH(OH)Et (0.024; 0.026), $EtCH_2CHO$ (0.008; 0.007), $EtCH_2CH_2OH$ (0.0012; 0.0042), $EtCH_2COOH$ (0.001; 0.001), acetic acid (0.0153; 0.0153)	980	18[d]
2	Propane	8	11	Acetone (0.0240; 0.0224), isopropanol (0.0874; 0.0920),*n*-propanol (0.0407; 0.0504), propanal (0.0063; 0.0072),propionic acid (0.0033; 0.0037), acetic acid (0.0048; 0.0042)	3500	8
3	Ethane	30	41	Ethanol (0.0426; 0.065), acetaldehyde (0.075; 0.056), acetic acid (0.051; 0.058)	3600	8
4	Methane	35	48	Methanol (0.0038; 0.009), formaldehyde (0.0018; 0.0017),acetic acid (0.0033; 0.0037)	214	0.5

[a] Reaction conditions: $[\mathbf{1}]_0 = 5 \times 10^{-5}$ M, $[H_2O_2]_0 = 2.2$ M, $[H_2O]_{total} = 4.2$ M, [py] = 0.1 M, 50 °C, 24 h. Total volume of the autoclave was 39 mL, volume of the reaction solution was 5 mL, and initial air pressure was 1 atm. In entry 4, acetic acid is formed exclusively *via* hydrolysis of acetonitrile.

[b] Concentrations of the products are given in brackets (the first value is concentration measured before reduction with PPh_3; the second value is after reduction with PPh_3).

[c] Based on H_2O_2.

[d] Based on *n*-butane.

from the results presented above, the rate constant of pseudo-first order for the reaction of $HO^{\cdot}$ with cyclohexane, $(0.4 \div 0.6) \times 10^9\ s^{-1}$, under our conditions is much higher in comparison with the corresponding constant for the reaction with H_2O_2 ($\leqslant 10^8\ s^{-1}$). We can, however, easily describe the dependence shown in Fig. 9B if we assume that an osmium-containing species "Os" reacts with hydrogen peroxide to form a peroxo complex "OsH_2O_2" (Eq. (4)). This complex decomposes to generate the hydroxyl radical (Eq. (5)).

$$\text{“Os”} + H_2O_2 \rightleftarrows \text{“}OsH_2O_2\text{”} \quad K_4 \tag{4}$$

$$\text{“}OsH_2O_2\text{”} \rightarrow HO^{\cdot} \quad k_5 \tag{5}$$

Taking into account that at $[\text{cyclohexane}]_0 = 0.46$ M practically all hydroxyl radicals in the quasi-equilibrium approximation in relation to "OsH_2O_2" are accepted by the alkane, we obtain the following equation:

$$W_{max} = -\frac{d[\text{cyclohexane}]}{dt} = \frac{k_5K_4[\text{“Os”}][H_2O_2]}{1 + K_4[H_2O_2]} \tag{6}$$

It follows from the data shown in Fig. 9B that at $[H_2O_2]_0 = 1$ M the alkane oxidation rate is equal to half of the maximum rate ($8 \times 10^{-6}\ M\ s^{-1}$). Using this value and Eq. (6), we can calculate the equilibrium constant (at 50 °C in acetonitrile containing 4.2 M H_2O) as $K_4 = 1\ M^{-1}$.

Hydroxyl radicals are apparently generated in the reaction between hydrogen peroxide and a 'low-valent' osmium derivative, most probably Os(II):

$$Os(II) + H_2O_2 \rightarrow Os(III) + HO^{\cdot} + HO^{-} \tag{7}$$

The Os(III) derivative thus formed can be reduced with a new molecule of H_2O_2 back to Os(II):

$$Os(III) + H_2O_2 \rightarrow Os(II) + HOO^{\cdot} + H^{+} \tag{8}$$

Other Os(*n*)–Os(*n* + 1) manifolds can also operate in such cycles, for example, we cannot exclude the participation of the Os(III)–Os(IV) pair. Hydroxyl radicals attack C–H bonds in accordance with equation:

$$RH + HO^{\cdot} \rightarrow R^{\cdot} + H_2O \tag{9}$$

Alkyl radicals add rapidly molecular oxygen from atmosphere:

$$R^{\cdot} + O_2 \rightarrow ROO^{\cdot} \tag{10}$$

Peroxyl radicals can be reduced with a 'low-valent' osmium species, for example:

$$ROO^{\cdot} + Os(II) \rightarrow ROO^{-} + Os(III) \tag{11}$$

and after addition of a proton are transformed into the primary reaction product, alkyl hydroperoxide:

$$ROO^{-} + H^{+} \rightarrow ROOH \tag{12}$$

We have found that the $\mathbf{1}/H_2O_2/py$ system efficiently oxidizes benzene to phenol in yield 22% (based on starting benzene) after 5 h (Fig. 12). Styrene is oxidized to benzaldehyde in yield 24% (based on starting styrene) after 12 h (Fig. 13). As in the case of alkanes, the oxidations of unsaturated hydrocarbons proceed with lag periods. It has been shown earlier using the vanadate/pyra-

Table 3
Selectivity parameters in H_2O_2 oxidations of alkanes by certain catalytic systems.[a]

Entry	Catalytic system	C(1):C(2):C(3):C(4)	1°:2°:3°		*trans*/*cis*	
		n-Heptane	MCH	Isooctane	*cis*-1,2-DMCH	*trans*-1,2-DMCH
1	**1**/py	1:7:7:7	1:8:23	1:5:8	1.0	0.9
2	$Fe(SO_4)_2$[b]	1:5:5:4.5		1:3:6	1.3	1.2
3	VO_3^-/PCA[c]	1:6:7:5	1:9:37	1:4:9	0.75	0.8
4	VO_3^-/H_2SO_4[d]	1:7:7:6	1:7:26		0.86	0.90
5	$Ni(ClO_4)_2/L$[e,f]	1:6:7:6	1:7:15	1:2:4		
6	$Al(NO_3)_3$[g]	1:5:5:5	1:6:23	1:4:7	0.8	0.8
7	Ti-MMM-2[h]	1:9:7:6.5	1:6:113	1:4:30	0.9	0.9
8	TS-1/NaOH/MeCN[i]	1:8:8:8	1:6:21	1:1:3	0.86	0.94
9	Fe_2(HPTB)/PCA[j]	1:6:6:5	1:6:13	1:3.5:8		
10	$NaAuCl_4$[k]	1:35:25:23	1:116:255	1:10:240		
11	$[Mn_2L_2(O)_3]^{2+}/MeCO_2H$[e,l]	1:46:35:34	1:26:200	1:5:50	0.34	4.1
12	$[Mn_2L_2(O)_3]^{2+}/(COOH)_2$[e,m,n]	1:17:12:11	1:0.3:0.6	1:0.4:32	0.2	7.3
13	$Cu(NCCH_3)_4BF_4$[m,o]	1:14:9:13	1:0:41			
14	TS-1[p]	1:80:193:100	No products	No products	No products	No products
15	$\mathbf{Cu_4}$[m,q]	1:34:23:21	1:16:128		0.4	0.1

[a] Parameter C(1):C(2):C(3):C(4) is the relative normalized (taking into account the number of hydrogen atoms at each carbon) reactivities of hydrogen atoms at carbons 1, 2, 3, and 4 of the chain of *n*-heptane. Parameter 1°:2°:3° is the relative normalized reactivities of hydrogen atoms at primary, secondary, and tertiary carbons of methylcyclohexane and isooctane. Parameter *trans*/*cis* is the ratio of isomers of *tert*-alcohols with mutual *trans*- and *cis*-orientation of the methyl groups formed in the oxidation of *cis*- and *trans*-1,2-dimethylcyclohexane (DMCH). All parameters were measured after reduction of the reaction mixtures with triphenylphosphine before GC analysis and calculated based on the ratios of isomeric alcohols.

[b] See Ref. [45].

[c] For this system, see Ref. [46]. PCA is pyrazine-2-carboxylic acid.

[d] For this system, see Ref. [47].

[e] *L* is 1,4,7-trimethyl-1,4,7-triazacyclononane.

[f] For this system, see Ref. [48].

[g] For this system, see Ref. [49].

[h] For this system, see Ref. [50].

[i] For this system, see Ref. [51].

[j] Fe_2(HPTB) is complex $[Fe_2(HPTB)(\mu\text{-}OH)(NO_3)_2](NO_3)_2$, HPTB = N,N,N′,N′-tetrakis(2-benzimidazolylmethyl)-2-hydroxo-1,3-diaminopropane. For this system, see Ref. [52].

[k] For this system, see Ref. [53].

[l] For this system, see Refs. [54,55].

[m] *tert*-Butylhydroperoxide is used instead of H_2O_2.

[n] For this system, see Ref. [56].

[o] For this system, see Ref. [57].

[p] For this system, see Ref. [58].

[q] $\mathbf{Cu_4}$ is complex $[O{\subset}Cu_4\{N(CH_2CH_2O)_3\}_4(BOH)_4][BF_4]_2$. For this system, see Refs. [58–60].

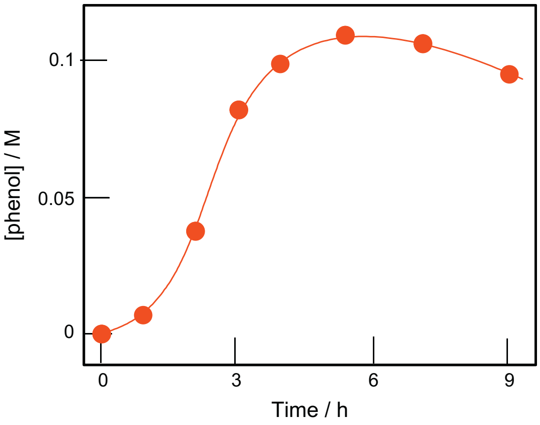

Fig. 12. Accumulation of phenol with time in the benzene oxidation with H_2O_2 catalyzed by complex **1** in the presence of pyridine in acetonitrile. Conditions: $[\mathbf{1}]_0 = 1 \times 10^{-4}$ M, $[\text{benzene}]_0 = 0.5$ M, $[H_2O_2]_0 = 1$ M, [py] = 0.05 M, 60 °C.

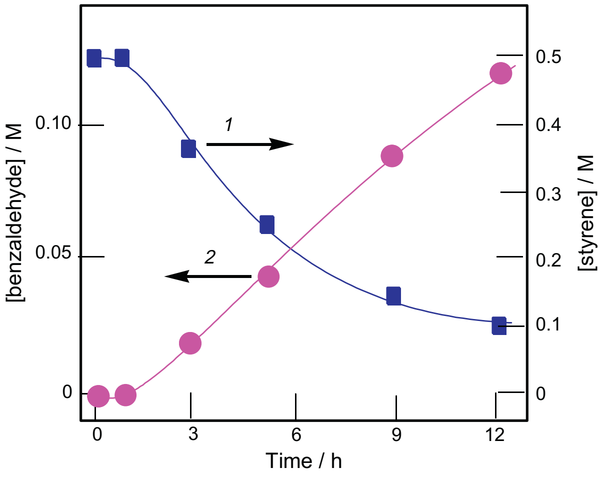

Fig. 13. Consumption of styrene (curve 1) and accumulation of benzaldehyde (curve 2) with time in styrene oxidation with H_2O_2 catalyzed by complex **1** in the presence of pyridine in acetonitrile. Conditions: $[\mathbf{1}]_0 = 1 \times 10^{-4}$ M, $[\text{styrene}]_0 = 0.5$ M, $[H_2O_2]_0 = 1$ M, [py] = 0.05 M, 60 °C.

zine-2-carboxylic acid/H_2O_2 system that the oxidation of benzene to phenol [64] and styrene to benzaldehyde [65] occurs with the participation of hydroxyl radicals.

We have also observed that the **1**/H_2O_2/py system oxidizes 1-phenylethanol to acetophenone. The reaction in the absence of pyridine affords only a negligible amount of acetophenone. However, in the presence of pyridine, the oxidation proceeds with auto-acceleration (Fig. 14). Heating a mixture of **1**, H_2O_2, pyridine, and acetonitrile during 1 h with subsequent addition of 1-phenylethanol led to removing the lag period (Fig. 15, curve 2). Incubation of the solution containing **1**, pyridine, 1-phenylethanol, and acetonitrile with subsequent addition of hydrogen peroxide reduced the lag period (Fig. 15, curve 3).

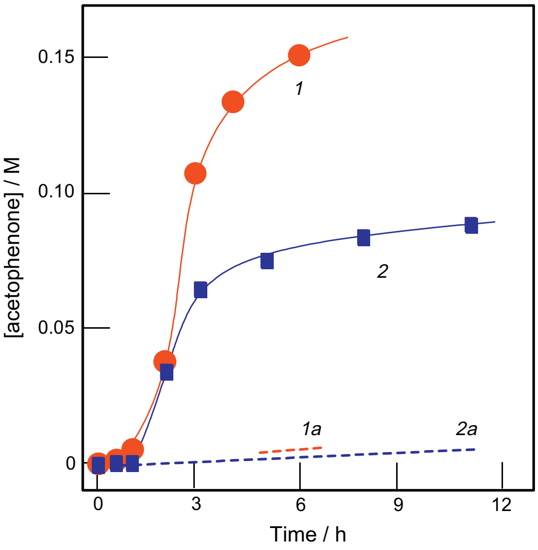

Fig. 14. Accumulation of acetophenone in the oxidation of 1-phenylethanol with H_2O_2 catalyzed by complex **1** at its different concentrations: $[\mathbf{1}]_0 = 5 \times 10^{-4}$ (curves 1 and 1*a*) and 1×10^{-4} M (curves 2 and 2*a*). Conditions: $[\text{1-phenylethanol}]_0 = 0.4$ M, $[H_2O_2]_0 = 1.0$ M, $[\text{pyridine}]_0 = 0.05$ M. Curves 1*a* and 2*a*: in the absence of pyridine. Solvent was acetonitrile (total volume of the reaction solution was 5 mL), 50 °C.

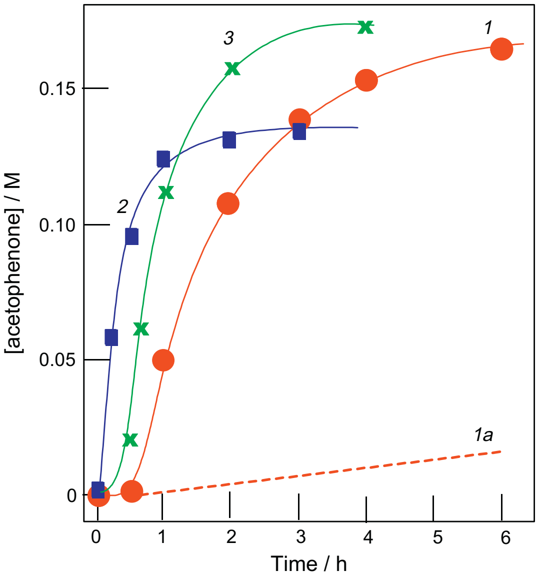

Fig. 15. Accumulation of acetophenone in the oxidation of 1-phenylethanol (0.4 M) with H_2O_2 (1.0 M) catalyzed by complex **1** (5×10^{-4} M (curves 1 and 1*a*) in the presence of pyridine (0.05 M). Curve 1a: the same in the absence of pyridine. Curve 2: the solution containing **1** (5×10^{-4} M), H_2O_2 (1.0 M), pyridine (0.05 M) and acetonitrile was incubated at 60 °C during 1 h. After that 1-phenylethanol (0.4 M) was added at the moment = 0 h. Curve 3: the solution containing **1** (5×10^{-4} M), pyridine (0.05 M), 1-phenylethanol (0.4 M), and acetonitrile was incubated at 60 °C during 1 h. After that H_2O_2 (1.0 M) was added at the moment = 0 h. Solvent was acetonitrile (total volume of the reaction solution was 5 mL), 60 °C.

A comparison of the data presented in Figs. 14 (curve 2) and 12 shows that the rate of 1-phenylethanol oxidation (2.7×10^{-5} M s^{-1}) is approximately three times higher than the rate of phenol accumulation (0.9×10^{-5} M s^{-1}) under similar conditions. As the benzene oxidation (as well as the oxidation of alkanes) is induced by hydroxyl radicals (see above), the difference in oxidation rates of 1-phenylethanol and benzene indicates that these substrates are oxidized with the participation of different intermediate species. One can assume that as in the case of catalysis by osmium carbonyl hydride [32], the oxidation of 1-phenylethanol catalyzed by **1** is induced by an osmyl species containing the "Os=O" moiety.

3. Conclusions

Decamethylosmocene very efficiently catalyzes the oxidation of alkanes with hydrogen peroxide in acetonitrile at 20–60 °C in the presence of pyridine. Turnover numbers, TONs, in the case of cyclohexane attain 51,000 (see Table 1, Entry 10), and maximum turnover frequency, TOF, was 6000 h^{-1} (see Fig. 5, curve 4*a*: maximum rate between 3 and 7 h). These values are much higher than TON and TOF parameters for other known alkane oxidizing systems. For example, copper-catalyzed oxidation by H_2O_2 proceeded with TOF of ca. 600 h^{-1}[59], oxidation catalyzed by a dinuclear manganese complex in the presence of oxalic acid exhibited TOF = 1200 h^{-1} [54], a vanadium complex in the presence of pyrazine-2-carboxylic acid gave TOF = 220 h^{-1} [46]. Finally, the oxidation of ethane by H_2O_2 in acetonitrile catalyzed by **1** in the presence of pyridine during 24 h gave the products with TON = 3600 and average TOF = 150 h^{-1} (see Table 2, Entry 3). For comparison, the $OsCl_3$-catalyzed oxidation of ethane by acetonitrile and water was much less efficient (TOF = 68 [33] and 41 h^{-1} [39], respectively). Decamethylosmocene **1** under the action of pyridine and hydrogen peroxide in acetonitrile is transformed into a catalytically active species, which decomposes hydrogen peroxide with formation of hydroxyl radicals. The role of pyridine is to accelerate the transformation of **1** into the catalytically active species. Hydroxyl radicals either abstract hydrogen atoms from alkanes to generate alkyl radicals or add to benzene rings or double bonds of styrene. Further reactions with molecular oxygen lead to the formation of primary products: alkyl hydroperoxides, phenol, or benzaldehyde, respectively.

4. Experimental

Caution. Due to the toxicity of osmium compounds, the heating oven should be located in a well-ventilated hood. The combination of air or molecular oxygen and H_2O_2 with organic compounds at elevated temperatures may be explosive!

Decamethylosmocene (pre-catalyst **1**) has been synthesized from Na_2OsCl_6 and pentamethylcyclopentadiene as described in Ref. [66]. The pre-catalyst **1** and pyridine were used in the form of stock solutions in acetonitrile. Aliquots of these solutions were added to the reaction mixtures in the oxidations of substrates. The oxidation reactions were typically carried out in air in thermostated Pyrex cylindrical vessels with vigorous stirring. The reactions with alkanes were stopped by cooling and analyzed twice, *i.e.*, before and after the addition of an excess of solid PPh_3. This method was developed and used previously by some of us [18,32,41,43,44] for the analysis of reaction mixtures obtained from various alkane oxidations. Applying this method in the present work for the oxidation of cyclohexane, we demonstrate that the reaction affords predominantly cyclohexyl hydroperoxide as the primary product, which slowly decomposes to form cyclohexanol and cyclohexanone. In our kinetic studies for precise determination of oxygenate concentrations, only data obtained after reduction of the reaction sample with PPh_3 were used. A Perkin Elmer Clarus 500 gas chromatograph with a capillary column 30 m × 0.22 mm × 25 μm, BP20 (SGE) was used (helium was the carrier gas; FID; the internal standard was nitromethane).

The oxidations of gaseous alkanes and/or oxidations in an O_2 or CO_2 atmosphere were carried out in a 39-mL stainless steel autoclave, equipped with a Teflon-coated magnetic stirring bar. In a typical experiment, after additions of all liquid reagents in the form of stock solutions in acetonitrile, the autoclave was closed and pressurized with 1.0–35.0 atm of gaseous alkane (typically 35.0, 30.0, 8.0, or 1.0 atm of CH_4, C_2H_6, C_3H_8, or n-C_4H_{10}, respectively) and/or O_2 (1.5 atm) or CO_2 (3 atm). The reaction mixture was stirred for 4–28 h at 50 °C using a magnetic stirrer and an oil bath, whereupon it was cooled in an ice bath, degassed, opened, and transferred to a flask for GC analysis.

Concentrations of the products obtained in the oxidation of benzene, styrene, and 1-phynylethanol after certain time intervals were measured using ^{1}H NMR method (acetone-d_6 was added to the samples; "Bruker AMX-400" instrument, 400 MHz). For the determination of concentrations of substrates and products, corresponding signals were integrated using added 1,4-dinitrobenzene as a standard.

Acknowledgments

The authors thank the Fundação para a Ciência e a Tecnologia (FCT) and its programmes (FEDER funded) (Grant BPD/34926/07 for M.V. K.) for support. G.B. S. and L.S. S. express their gratitude to the FCT for making it possible for them to stay at the Instituto Superior Técnico, TU Lisbon, as invited scientists and to perform a part of the present work.

References

[1] M. Beller, C. Bolm (Eds.), Transition Metals for Organic Synthesis, second ed., Wiley-VCH, Weinheim, Germany, 2004.
[2] G. Tojo, M. Fernandez, Oxidation of Alcohols to Aldehydes and Ketones, Springer Science, Business Media, Inc., New York, 2006.
[3] T. Seki, A. Baiker, Chem. Rev. 109 (2009) 2409–2454.
[4] Z. Ye, Z. Fu, S. Zhong, F. Xie, X. Zhou, F. Liu, D. Yin, J. Catal. 261 (2009) 110–115.
[5] P.J. Figiel, J.M. Sobczak, J. Catal. 263 (2009) 167–172.
[6] L.S. Shul'pina, K. Takaki, T.V. Strelkova, G.B. Shul'pin, Petrol. Chem. 48 (2008) 219–222.
[7] N.K. Renuka, J. Mol, Catal. A: Chem. 316 (2010) 126–130.
[8] S.T. Oyama (Ed.), Mechanisms in Homogeneous and Heterogeneous Epoxidation, Elsevier, 2008.
[9] M. Vasconcellos-Dias, C.D. Nunes, P.D. Vaz, P. Ferreira, P. Brandão, V. Félix, M.J. Calhorda, J. Catal. 256 (2008) 301–311.
[10] A. Corma, I. Domínguez, A. Doménech, V. Fornés, C.J. Gómez-García, T. Ródenas, M.J. Sabater, J. Catal. 265 (2009) 238–244.
[11] G.A.E. Oxford, M.C. Curet-Arana, D. Majumder, R.W. Gurney, M.L. Merlau, S.T. Nguyen, R.Q. Snurr, L.J. Broadbelt, J. Catal. 266 (2009) 145–155.
[12] D. Jiang, T. Mallat, D.M. Meier, A. Urakawa, A. Baiker, J. Catal. 270 (2010) 26–33.
[13] J.M. Escola, J.A. Botas, C. Vargas, M. Bravo, J. Catal. 270 (2010) 34–39.
[14] M.G. Buonomenna, G. Golemme, M.P. De Santo, E. Drioli, Org. Proc. Res. Develop. 14 (2010) 252–258.
[15] T.R. Amarante, P. Neves, A.C. Coelho, S. Gago, A.A. Valente, F.A.A. Paz, M. Pillinger, I.S. Gonçalves, Organometallics 29 (2010) 883–892.
[16] A.E. Shilov, G.B. Shul'pin, Chem. Rev. 97 (1997) 2879–2932.
[17] A.E. Shilov, G.B. Shul'pin, Activation and Catalytic Reactions of Saturated Hydrocarbons in the Presence of Metal Complexes, Dordrecht, Kluwer Academic Publishers, 2000.
[18] G.B. Shul'pin, Mini-Rev. Org. Chem. 6 (2009) 95–104.
[19] G.B. Shul'pin, Org. Biomol. Chem. 8 (2010) 4217–4228.
[20] G.S. Nunes, A.D.P. Alexiou, H.E. Toma, J. Catal. 260 (2008) 188–192.
[21] G.S. Machado, G.G.C. Arizaga, F. Wypych, S. Nakagaki, J. Catal. 274 (2010) 130–141.
[22] U. Schuchardt, D. Mandelli, G.B. Shul'pin, Tetrahedron Lett. 37 (1996) 6487–6490.
[23] G.B. Shul'pin, D.V. Muratov, L.S. Shul'pina, A.R. Kudinov, T.V. Strelkova, P.V. Petrovskiy, Appl. Organometal. Chem. 22 (2008) 684–688.
[24] R. Saladino, V. Nery, A. Farina, C. Crestini, L. Nencioni, A.T. Palamara, Adv. Synth. Catal. 350 (2008) 321–331.
[25] M.L. Kuznetsov, A.J.L. Pombeiro, Inorg. Chem. 48 (2009) 307–318.
[26] E.A. Karlsson, T. Privalov, Chem. Eur. J. 15 (2009) 1862–1869.
[27] P.F. Oblad, J.E. Bercaw, N. Hazari, J.A. Labinger, Organometallics 29 (2010) 789–794.
[28] A. Dehestani, A. Wu, R. Hayoun, W. Kaminsky, J.M. Mayer, Inorg. Chim. Acta 362 (2009) 4534–4538.
[29] D.H. Ess, J. Org. Chem. 74 (2009) 1498–1508.
[30] D. Veghini, L.S. Shul'pina, T.V. Strelkova, G.B. Shul'pin, Petrol. Chem. 46 (2006) 167–170.
[31] L.S. Shul'pina, D. Veghini, A.R. Kudinov, G.B. Shul'pin, React. Kinet. Catal. Lett. 88 (2006) 157–164.
[32] G.B. Shul'pin, Y.N. Kozlov, L.S. Shul'pina, P.V. Petrovskiy, Appl. Organometal. Chem. 24 (2010) 464–472.
[33] G.B. Shul'pin, G. Süss-Fink, L.S. Shul'pina, Chem. Commun. (2000) 1131–1132.
[34] G.B. Shul'pin, G. Süss-Fink, Petrol. Chem. 42 (2002) 233–237.
[35] T. Osako, E.J. Watson, A. Dehestani, B.C. Bales, J.M. Mayer, Angew. Chem. Int. Ed. 45 (2006) 7433–7436.
[36] G.B. Shul'pin, A.R. Kudinov, L.S. Shul'pina, E.A. Petrovskaya, J. Organometal. Chem. 691 (2006) 837–845.
[37] L.S. Shul'pina, A.R. Kudinov, E.A. Petrovskaya, T.V. Strelkova, G.B. Shul'pin, Petrol. Chem. 46 (2006) 164–166.
[38] S. Ogawa, K. Hosoi, T. Iida, Y. Wakatsuki, M. Makino, Y. Fujimoto, A.F. Hofmann, Eur. J. Org. Chem. 10 (2007) 3555–3563.
[39] Q. Yuan, W. Deng, Q. Zhang, Y. Wang, Adv. Synth. Catal. 349 (2007) 1199–1209.
[40] S.-M. Yiu, W.-L. Man, T.-C. Lau, J. Am. Chem. Soc. 130 (2008) 10821–10827.
[41] G.B. Shul'pin, Y.N. Kozlov, L.S. Shul'pina, A.R. Kudinov, D. Mandelli, Inorg. Chem. 48 (2009) 10480–10482.
[42] S. Ogawa, Y. Wakatsuki, M. Makino, Y. Fujimoto, K. Yasukawa, T. Kikuchi, M. Ukiya, T. Akihisa, T. Iida, Chem. Phys. Lipids 163 (2010) 165–171.
[43] G.B. Shul'pin, J. Mol, Catal. A: Chem. 189 (2002) 39–66.
[44] G.B. Shul'pin, Comptes Rendus, Chimie 6 (2003) 163–178.
[45] G.B. Shul'pin, G.V. Nizova, Y.N. Kozlov, L. Gonzalez Cuervo, G. Süss-Fink, Adv. Synth. Catal. 346 (2004) 317–332.
[46] M.V. Kirillova, M.L. Kuznetsov, V.B. Romakh, L.S. Shul'pina, J.J.R. Fraústo da Silva, A.J.L. Pombeiro, G.B. Shul'pin, J. Catal. 267 (2009) 140–157.
[47] L.S. Shul'pina, M.V. Kirillova, A.J.L. Pombeiro, G.B. Shul'pin, Tetrahedron 65 (2009) 2424–2429.
[48] G.B. Shul'pin, J. Chem. Res. (2002) 351–353.
[49] D. Mandelli, K.C. Chiacchio, Y.N. Kozlov, G.B. Shul'pin, Tetrahedron Lett. 49 (2008) 6693–6697.
[50] A.J. Bonon, D. Mandelli, O.A. Kholdeeva, M.V. Barmatova, Y.N. Kozlov, G.B. Shul'pin, Appl. Catal. A: Gen. 365 (2009) 96–104.
[51] G.B. Shul'pin, M.V. Kirillova, T. Sooknoi, A.J.L. Pombeiro, Catal. Lett. 128 (2008) 135–141.
[52] G.V. Nizova, B. Krebs, G. Süss-Fink, S. Schindler, L. Westerheide, L. Gonzalez Cuervo, G.B. Shul'pin, Tetrahedron 58 (2002) 9231–9237.
[53] G.B. Shul'pin, G. Süss-Fink, A.E. Shilov, Tetrahedron Lett. 42 (2001) 7253–7256.
[54] G.B. Shul'pin, M.G. Matthes, V.B. Romakh, M.I.F. Barbosa, J.L.T. Aoyagi, D. Mandelli, Tetrahedron 64 (2008) 2143–2152.
[55] G.B. Shul'pin, Y.N. Kozlov, S.N. Kholuiskaya, M.I. Plieva, J. Mol, Catal. A: Chem. 299 (2009) 77–87.
[56] Y.N. Kozlov, G.V. Nizova, G.B. Shul'pin, J. Phys. Org. Chem. 21 (2008) 119–126.
[57] G.B. Shul'pin, J. Gradinaru, Y.N. Kozlov, Org. Biomol. Chem. 1 (2003) 3611–3617.
[58] G.B. Shul'pin, T. Sooknoi, V.B. Romakh, G. Süss-Fink, L.S. Shul'pina, Tetrahedron Lett. 47 (2006) 3071–3075.
[59] M.V. Kirillova, Y.N. Kozlov, L.S. Shul'pina, O.Y. Lyakin, A.M. Kirillov, E.P. Talsi, A.J.L. Pombeiro, G.B. Shul'pin, J. Catal. 268 (2009) 26–38.
[60] M.V. Kirillova, A.M. Kirillov, D. Mandelli, W.A. Carvalho, A.J.L. Pombeiro, G.B. Shul'pin, J. Catal. 272 (2010) 9–17.
[61] Y.N. Kozlov, G.V. Nizova, G.B. Shul'pin, J. Mol, Catal. A: Chem. 227 (2005) 247–253.
[62] G. Süss-Fink, G.V. Nizova, S. Stanislas, G.B. Shul'pin, J. Mol, Catal. A: Chem. 130 (1998) 163–170.
[63] P. Neta, R.E. Huie, A.B. Ross, J. Phys, Chem. Ref. Data 17 (1988) 1027–1284.
[64] M.H.C. de la Cruz, Y.N. Kozlov, E.R. Lachter, G.B. Shul'pin, New J. Chem. 27 (2003) 634–638.
[65] G.B. Shul'pin, Y. Ishii, S. Sakaguchi, T. Iwahama, Russ. Chem. Bull. 48 (1999) 887–890.
[66] D.C. Liles, A. Shaver, E. Singleton, M.B. Wiege, J. Organometal. Chem. 288 (1985) C33–C36.